Flutter of Coaxial Cylindrical Shells in an Incompressible Axisymmetric Flow

THOMAS S. DAVID*
Consultants & Designers Inc., East Hartford, Conn.
AND
A. V. SRINIVASAN†
Pratt & Whitney Aircraft, East Hartford, Conn.

The coalescence type of flutter of a long rotating cylindrical shell with its outer surface exposed to a general inviscid, incompressible, fully developed (axially), axisymmetric flow with vanishing radial velocity component is considered. The flow is governed by perturbation theory. The cylinder response is described by classical shell equations. Analytical solutions are obtained for the special cases of flows with uniform axial velocity, but the tangential velocity is: 1) represented by a coaxial, potential vortex, or 2) varying linearly with radius. Numerical solutions are presented for more general flows. The flutter speed and flutter frequency are compared with available experimental data.

Nomenclature

a = radius of inner shell
a_1, a_2 = arbitrary constants in the solution to $f(r)$
A = $V^s/r + \partial V^s/\partial r$
b = radius of outer shell
B = $\left(\frac{\partial}{\partial t} + \frac{V^s}{r}\frac{\partial}{\partial \theta} + U^s\frac{\partial}{\partial z}\right)$
C^* = see Eq. (22)
C_0 = $(E_1/\rho_{m_1})^{1/2}$
d = $\frac{\lambda^2}{\alpha^2}[-\alpha^2 + 4k^2]$ [see Eq. (26)]
d_{ij} = see Eq. (22)
E = Young's modulus
$f(r)$ = amplitude of perturbed pressure
f_1, f_2 = solutions of $f(r)$
h = shell thickness
k = special tangential velocity profile constant ($V^s = k/r, kr$)
l = length of shell
$[L]$ = linear operator in shell equation [see Eq. (21)]
L_{ij} = elements of $[L]$
L_{ij}^{-1} = corresponding elements of the inverse of $[L]$
m = number of half waves in the axial direction
n = number of circumferential waves
p = fluid pressure
r, θ, z = cylindrical coordinates
s = surface of shell
t = time coordinate
U, V, W = velocity of fluid in the axial, tangential, and radial directions, respectively
u, v, w = displacement of an element of shell in the axial, tangential, and radial directions, respectively
$\hat{u}, \hat{v}, \hat{w}$ = constant amplitudes of $u. v. w$
$\alpha(r)$ = $\left[\omega + \frac{V^s}{r}n + U^s\lambda\right]$
β = $n\theta + \lambda z + \omega t$
δ = b/a
δ_1 = a/h_1
δ_2 = b/h_2
ρ_m = shell density
ρ_∞ = fluid density
σ = E_1/E_2
λ = $m\pi/l_1$
ν = Poisson's ratio
ω = frequency of oscillation in radians/sec
Ω = angular velocity of shell in radians/sec
∇^2 = Laplacian in cylindrical coordinates
Δ_{ij} = element of flutter determinant
$\tilde{(\ )}$ = perturbed quantity
$(\ )^s$ = steady quantity
$(\ )^*$ = nondimensional quantity
$(\ )_1$ = refers to inner shell
$(\ )_2$ = refers to outer shell

Introduction

THE problem of aeroelastic stability of traveling waves on a thin-walled nonrotating cylinder subject to an axial flow on its outer surface has been studied theoretically by Leonard and Hedgepeth,[1] Miles,[2] Bolotin,[3] and Dowell.[4] Srinivasan[5] investigated the problem for a rotating cylinder in a compressible flow that has, in addition to axial flow, a tangential velocity component. The waves are assumed to travel both axially and circumferentially. The tangential velocity was assumed to be that of a coaxial potential vortex, hence the flowfield could be represented by a velocity potential. The present paper considers the problem where the flow is inviscid and incompressible, but the axial and tangential velocities can have a general profile.

Such investigation is of interest in the design of rotor systems of jet engines where the swirling flow around a rotor is likely to be of the general type. An experimental study of this problem is reported in Ref. 8.

Formulation

The geometrical model which forms the basis for this analytical study is shown in Fig. 1. The fluid is contained within the annulus between two rotating flexible thin cylinders of radii a and b.

Received January 31, 1974; revision received July 29, 1974. The authors wish to thank the Management of Pratt & Whitney Aircraft for permitting the publication of the contents of this paper; K. Brown, Technical and Research Engineering, Pratt & Whitney Aircraft, for his assistance in obtaining the computed data; and E. Dowell, Princeton University, for his helpful suggestions during the preparation of this paper.

Index category: Aeroelasticity and Hydroelasticity.

* Senior Research Engineer.

† Senior Assistant Project Engineer, Technical and Research Engineering, Pratt & Whitney Aircraft Division of United Aircraft Corporation.

Governing Flow Equations

The fluid is assumed to be incompressible and inviscid. Under this assumption, the momentum and continuity equations for the flow in cylindrical coordinates are as follows:

$$\rho_\infty\left[\frac{\partial W}{\partial t}+W\frac{\partial W}{\partial r}+\frac{V}{r}\frac{\partial W}{\partial \theta}+U\frac{\partial W}{\partial z}-\frac{V^2}{r}\right]=-\frac{\partial p}{\partial r} \quad (1)$$

$$\rho_\infty\left[\frac{\partial V}{\partial t}+W\frac{\partial V}{\partial r}+\frac{V}{r}\frac{\partial V}{\partial \theta}+U\frac{\partial V}{\partial z}+\frac{WV}{r}\right]=-\frac{1}{r}\frac{\partial p}{\partial \theta} \quad (2)$$

$$\rho_\infty\left[\frac{\partial U}{\partial t}+W\frac{\partial U}{\partial r}+\frac{V}{r}\frac{\partial U}{\partial \theta}+U\frac{\partial U}{\partial z}\right]=-\frac{\partial p}{\partial z} \quad (3)$$

$$\frac{\partial W}{\partial r}+\frac{1}{r}W+\frac{1}{r}\frac{\partial V}{\partial \theta}+\frac{\partial U}{\partial z}=0 \quad (4)$$

Let $U=U^s+\tilde{u}$, $V=V^s+\tilde{v}$, $W=W^s+\tilde{w}$, $p=p^s+\tilde{p}$, and $\rho_\infty=\rho_\infty$ where $(\ )^s$ is steady part and $(\tilde{\ })$ the perturbed part. For steady state

$$\frac{\partial(\ )^s}{\partial t}=0$$

$$\frac{\partial(\ )^s}{\partial \theta}=0 \quad \text{(axisymmetric)} \quad (5)$$

$$\frac{\partial(\ )^s}{\partial z}=0 \quad \text{(fully developed, axially)}$$

We also assume that $W^s=0$ (small compared with U^s or V^s).

Using Eq. (5) and neglecting second-order terms in the perturbed quantities, we get from the momentum and continuity equations

$$\rho_\infty\left[\frac{\partial \tilde{w}}{\partial t}+\frac{V^s}{r}\frac{\partial \tilde{w}}{\partial \theta}+U^s\frac{\partial \tilde{w}}{\partial z}-2\frac{V^s\tilde{v}}{r}\right]=-\frac{\partial \tilde{p}}{\partial r} \quad (6)$$

$$\rho_\infty\left[\frac{\partial \tilde{v}}{\partial t}+\tilde{w}\frac{\partial V^s}{\partial r}+\frac{V^s}{r}\frac{\partial \tilde{v}}{\partial \theta}+U^s\frac{\partial \tilde{v}}{\partial z}+\frac{\tilde{w}V^s}{r}\right]=-\frac{1}{r}\frac{\partial \tilde{p}}{\partial \theta} \quad (7)$$

$$\rho_\infty\left[\frac{\partial \tilde{u}}{\partial t}+\tilde{w}\frac{\partial U^s}{\partial r}+\frac{V^s}{r}\frac{\partial \tilde{u}}{\partial \theta}+U^s\frac{\partial \tilde{u}}{\partial z}\right]=-\frac{\partial \tilde{p}}{\partial z} \quad (8)$$

$$\frac{\partial \tilde{w}}{\partial r}+\frac{1}{r}\tilde{w}+\frac{1}{r}\frac{\partial \tilde{v}}{\partial \theta}+\frac{\partial \tilde{u}}{\partial z}=0 \quad (9)$$

Eliminating $\tilde{u}$, $\tilde{v}$, and $\tilde{w}$ from the last four equations (see Appendix), we get for the perturbed pressure, $\tilde{p}$, the governing equation

$$2\frac{(V^s)^2}{r^3}\left(\frac{\partial A}{\partial r}\right)\left(B\frac{\partial \tilde{p}}{\partial \theta}\right)-\frac{1}{2}(B^4\nabla^2\tilde{p})-\frac{V^s}{r}A(B^2\nabla^2\tilde{p})+$$
$$\frac{V^s}{r}\frac{\partial^2 V^s}{\partial r^2}\left(B^2\frac{\partial \tilde{p}}{\partial r}\right)+\frac{A}{r}\frac{\partial V^s}{\partial r}\left(B^2\frac{\partial \tilde{p}}{\partial r}\right)-2\frac{(V^s)^2}{r^3}\left(B^2\frac{\partial \tilde{p}}{\partial r}\right)-$$
$$2\frac{(V^s)^2}{r^2}A^2\frac{\partial^2 \tilde{p}}{\partial z^2}-\frac{V^s}{r}A\left(B^2\frac{\partial^2 \tilde{p}}{\partial z^2}\right)+\frac{(V^s)^2}{r^3}\cdot\frac{\partial\left(\frac{V^s}{r}\right)}{\partial r}\cdot$$
$$\left(B\frac{\partial^3 \tilde{p}}{\partial \theta^3}\right)+2\frac{(V^s)^2}{r^3}\frac{\partial U^s}{\partial r}A\frac{\partial^2 \tilde{p}}{\partial \theta\,\partial z}+3\frac{V^s}{r^2}\frac{\partial U^s}{\partial r}\left(B^2\frac{\partial^2 \tilde{p}}{\partial \theta\,\partial z}\right)+$$
$$\frac{\partial U^s}{\partial r}\left(B^3\frac{\partial^2 \tilde{p}}{\partial r\,\partial z}\right)+\frac{\partial\left(\frac{V^s}{r}\right)}{\partial r}\left(B^3\frac{\partial^2 \tilde{p}}{\partial r\,\partial \theta}\right)-$$
$$\frac{1}{r}\frac{\partial\left(\frac{V^s}{r}\right)}{\partial r}(U^s)^2\left(B\frac{\partial^3 \tilde{p}}{\partial z^2\,\partial \theta}\right)-\frac{2}{r}\frac{\partial\left(\frac{V^s}{r}\right)}{\partial r}U^s\left(B\frac{\partial^3 \tilde{p}}{\partial t\,\partial \theta\,\partial z}\right)-$$
$$\frac{1}{r}\frac{\partial\left(\frac{V^s}{r}\right)}{\partial r}\left(B\frac{\partial^3 \tilde{p}}{\partial t^2\,\partial \theta}\right)=0 \quad (10)$$

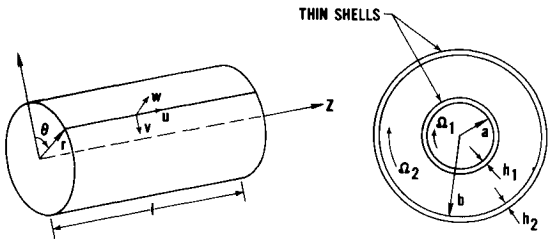

Fig. 1 Mathematical model.

where

$$A\equiv\left(\frac{V^s}{r}+\frac{\partial V^s}{\partial r}\right)$$

$$B\equiv\left(\frac{\partial}{\partial t}+\frac{V^s}{r}\frac{\partial}{\partial \theta}+U^s\frac{\partial}{\partial z}\right)$$

$$\nabla^2\equiv\left(\frac{\partial^2}{\partial r^2}+\frac{1}{r}\frac{\partial}{\partial r}+\frac{1}{r^2}\frac{\partial^2}{\partial \theta^2}+\frac{\partial^2}{\partial z^2}\right)$$

Equation (10) is the required differential equation for $\tilde{p}$.

Boundary Conditions

Equation (10) is second order in r and thus we need two boundary conditions on $\tilde{p}$ in the r direction. These boundary conditions are

$$DS/Dt=0 \quad \text{at} \quad r=a,b \quad (11)$$

where S = surface of shell and D/Dt = derivative (total). After developing Eq. (11) to the first order in the perturbed quantities, we get

$$\tilde{w}=\left[\frac{\partial w_1}{\partial t}+\frac{V^s}{r}\frac{\partial w_1}{\partial \theta}+U^s\frac{\partial w_1}{\partial z}\right] \quad \text{at} \quad r=a$$
$$\tilde{w}=\left[\frac{\partial w_2}{\partial t}+\frac{V^s}{r}\frac{\partial w_2}{\partial \theta}+U^s\frac{\partial w_2}{\partial z}\right] \quad \text{at} \quad r=b \quad (12)$$

where w_1, w_2 are radial displacement of the inner and outer shell, respectively. Equations (6) and (7) can be written as

$$\rho_\infty[B]\tilde{w}-2\rho_\infty(V^s/r)\tilde{v}=-(\partial\tilde{p}/\partial r) \quad (13)$$

$$\rho_\infty[B]\tilde{v}+\rho_\infty A\tilde{w}=-(1/r)(\partial\tilde{p}/\partial\theta) \quad (14)$$

Equation (12) can be written as

$$\tilde{w}=[B]w_1 \quad \text{at} \quad r=a$$
$$\tilde{w}=[B]w_2 \quad \text{at} \quad r=b \quad (15)$$

From Eqs. (15) and (13)

$$\rho_\infty[B]^2w_1-2\rho_\infty\frac{V^s}{r}\tilde{v}=-\frac{\partial\tilde{p}}{\partial r} \quad \text{at} \quad r=a$$
$$\rho_\infty[B]^2w_2-2\rho_\infty\frac{V^s}{r}\tilde{v}=-\frac{\partial\tilde{p}}{\partial r} \quad \text{at} \quad r=b \quad (16)$$

From Eqs. (15) and (14)

$$\rho_\infty[B]\tilde{v}=-\rho_\infty A[B]w_1-\frac{1}{r}\frac{\partial\tilde{p}}{\partial\theta} \quad \text{at} \quad r=a$$
$$\rho_\infty[B]\tilde{v}=-\rho_\infty A[B]w_2-\frac{1}{r}\frac{\partial\tilde{p}}{\partial\theta} \quad \text{at} \quad r=b \quad (17)$$

Substituting $\tilde{v}$ from Eq. (17) into Eq. (16), and noting Eq. (5), we get

$$\rho_\infty[B]^3w_1+\frac{2\rho_\infty}{a}V^sA[B]w_1=-2\frac{V^s}{a^2}\frac{\partial\tilde{p}}{\partial\theta}-[B]\frac{\partial\tilde{p}}{\partial r} \quad \text{at} \quad r=a$$
$$\rho_\infty[B]^3w_2+\frac{2\rho_\infty}{b}V^sA[B]w_2=-2\frac{V^s}{b^2}\frac{\partial\tilde{p}}{\partial\theta}-[B]\frac{\partial\tilde{p}}{\partial r} \quad \text{at} \quad r=b \quad (18)$$

Equations (18) are the two boundary conditions on $\tilde{p}$ in the r-direction. Equation (10) has to be solved subject to the boundary conditions of Eq. (18).

Class of Solutions

We now consider solutions to Eq. (10), Eq. (18) of the class described by

$$\left.\begin{aligned} u_1 &= \hat{u}_1 e^{i\beta} \\ v_1 &= \hat{v}_1 e^{i\beta} \\ w_1 &= \hat{w}_1 e^{i\beta} \end{aligned}\right\} \quad \left.\begin{aligned} u_2 &= \hat{u}_2 e^{i\beta} \\ v_2 &= \hat{v}_2 e^{i\beta} \\ w_2 &= \hat{w}_2 e^{i\beta} \end{aligned}\right\} \quad \tilde{p} = f(r)e^{i\beta} \tag{19}$$

with $\beta = n\theta + \lambda z - \omega t$, with $\lambda = m\pi/l_1$ and where l_1 = length of inner cylindrical shell, n = tangential wave number, m = axial half-wave number, and ω = frequency of vibration. Also, u, v, and w represent the axial, tangential, and radial displacement of shell, $\hat{u}$, $\hat{v}$, and $\hat{w}$ are constants, and $(\ )_1$, and $(\ )_2$ stand for the inner and outer shell, respectively.

Nondimensionalization

We nondimensionalize with the following quantities: velocity: $C_0 \equiv (E_1/\rho_{m_1})^{1/2}$ where E_1 = modulus of elasticity of inner shell; ρ_{m_1} = density of inner shell; length: a = radius of inner shell; pressure: E_1; time: a/C_0; and density: ρ_{m_1}. In what follows we retain the same notation for the now nondimensional quantities.

Introducing the class of solutions of Eq. (19), we get from Eqs. (10) and (18) in nondimensional form

$$\left\{-\frac{1}{2}\alpha^4 + \frac{V^s}{r}A\alpha^2\right\}f'' + \left\{-\frac{1}{2r}\alpha^4 + \frac{V^s}{r^2}A\alpha^2 - \frac{V^s}{r}\frac{\partial^2 V^s}{\partial r^2}\alpha^2 - \frac{A}{r}\frac{\partial V^s}{\partial r}\alpha^2 + 2\frac{(V^s)^2}{r^3}\alpha^2 + \frac{\partial U^s}{\partial r}\lambda\alpha^3 + \frac{\partial\left(\frac{V^s}{r}\right)}{\partial r}n\alpha^3\right\}f' +$$

$$\left\{-2\frac{(V^s)^2}{r^3}\left(\frac{\partial A}{\partial r}\right)n\alpha + \frac{1}{2}\frac{n^2}{r^2}\alpha^4 + \frac{1}{2}\lambda^2\alpha^4 - \frac{n^2}{r^3}V^sA\alpha^2 - \frac{\lambda^2}{r}V^sA\alpha^2 + 2\frac{(V^s)^2}{r^2}A^2\lambda^2 - \frac{\lambda^2}{r}V^sA\alpha^2 + \frac{n^3\alpha(V^s)^2}{r^3}\frac{\partial\left(\frac{V^s}{r}\right)}{\partial r} - \frac{2n\lambda}{r^3}A(V^s)^2\frac{\partial U^s}{\partial r} + \frac{3n\lambda\alpha^2}{r^2}V^s\frac{\partial U^s}{\partial r} - \frac{n\lambda^2\alpha(U^s)^2}{r}\frac{\partial\left(\frac{V^s}{r}\right)}{\partial r} + \frac{2\omega n\lambda\alpha U^s}{r}\frac{\partial\left(\frac{V^s}{r}\right)}{\partial r} - \frac{\omega^2 n\alpha}{r}\frac{\partial\left(\frac{V^s}{r}\right)}{\partial r}\right\}f = 0 \tag{20}$$

and the boundary conditions

$$\begin{aligned} -\rho_\infty\alpha^3\hat{w}_1 + 2\rho_\infty V^sA\alpha\hat{w}_1 &= -2nV^sf(1) - \alpha f'(1) \quad \text{at} \quad r = 1 \\ -\rho_\infty\alpha^3\hat{w}_2 + \frac{2}{\delta}\rho_\infty V^sA\alpha\hat{w}_2 &= -\frac{2}{\delta^2}nV^sf(\delta) - \alpha f'(\delta) \quad \text{at} \quad r = \delta \end{aligned} \tag{21}$$

where $(\ )^1$ denotes differentiation with respect to r, $\delta = b/a$, and $\alpha(r) \equiv [-\omega + (V^s/r)n + U^s\lambda]$. Equation (20) has to be solved for $f(r)$ subject to the boundary conditions of Eq. (21).

Shell Equations

The usual assumptions of linear, elastic thin-shell theory are made for the shell equations. For a long thin cylindrical shell subjected to radial dynamic pressure, these equations are, in nondimensional form,[6]

$$\begin{aligned} [L_1]\begin{Bmatrix} u_1 \\ v_1 \\ w_1 \end{Bmatrix} &= \begin{Bmatrix} 0 \\ 0 \\ -\tilde{p} \end{Bmatrix} \quad \text{at} \quad r = 1 \\ [L_2]\begin{Bmatrix} u_2 \\ v_2 \\ w_2 \end{Bmatrix} &= \begin{Bmatrix} 0 \\ 0 \\ +\tilde{p} \end{Bmatrix} \quad \text{at} \quad r = \delta \end{aligned} \tag{22}$$

where L_1, L_2 are linear operators, L_{ij}. These operators include centrifugal and coriolis loadings due to rotation, and may also be found in Ref. 5.

Method of Solution

We note that Eqs. (20) and (21) together with Eq. (22) lead to an eigenvalue problem. Using Eq. (22), the boundary conditions on f [i.e., Eqs. (21)] can be written as

$$\begin{aligned} (C_1^* - d_{11})f(1) - d_{12}f'(1) &= 0 \quad \text{at} \quad r = 1 \\ (C_2^* - d_{21})f(\delta) - d_{22}f'(\delta) &= 0 \quad \text{at} \quad r = \delta \end{aligned} \tag{23}$$

where

$$\left.\begin{aligned} C_1^* &\equiv -[\rho_\infty\alpha^3 + 2\rho_\infty V^sA\alpha]L_{1_{33}}^{-1}(1-\nu_1^2)\delta_1 \\ d_{11} &\equiv -2nV^s \\ d_{12} &\equiv -\alpha \end{aligned}\right\} \text{at} \quad r = 1$$

$$\left.\begin{aligned} C_2^* &\equiv \left[-\rho_\infty\alpha^3 + \frac{2}{\delta}\rho_\infty V^sA\alpha\right]L_{2_{33}}(1-\nu_2^2)\delta_2\delta\sigma \\ d_{21} &\equiv -\frac{2}{\delta^2}nV^s \\ d_{22} &\equiv -\alpha \end{aligned}\right\} \text{at} \quad r = \delta$$

with $\delta_1 \equiv a/h_1$ where h_1 = thickness of inner shell, $\delta_2 \equiv b/h_2$ where h_2 = thickness of outer shell, $\sigma \equiv E_1/E_2$, and L_{ij}^{-1} are the corresponding elements of the inverse of $[L]$.

Let the solution of Eq. (20) be $f = a_1f_1 + a_2f_2$. A nontrivial solution for a_1 and a_2 requires the vanishing of the determinant in Eq. (23)

$$|\Delta_{ij}| = 0 \qquad i, j = 1, 2 \tag{24}$$

where

$$\begin{aligned} \Delta_{11} &= \{(C_1^* - d_{11})f_1(1) - d_{12}f_1'(1)\}_{r=1} \\ \Delta_{12} &= \{(C_1^* - d_{11})f_2(1) - d_{12}f_2'(1)\}_{r=1} \\ \Delta_{21} &= \{(C_2^* - d_{21})f_1(\delta) - d_{22}f_1'(\delta)\}_{r=\delta} \\ \Delta_{22} &= \{(C_2^* - d_{21})f_2(\delta) - d_{22}f_2'(\delta)\}_{r=\delta} \end{aligned}$$

If the frequency of vibration ω is real, the determinant of Eq. (24) is also real. Then the solution of Eq. (24) provides the eigenvalues. A typical plot of such eigenvalues is shown in Fig. 2.

Numerical Solution

The numerical analysis is essentially similar to that used in Ref. 5. Any two independent solutions f_1, f_2 to Eq. (20) are sought by prescribing the following arbitrary conditions at $r = 1$

$$\begin{aligned} f_1 &= 1 \quad f_1' = 0 \\ f_2 &= 0 \quad f_2' = 1 \end{aligned} \quad \text{at} \quad r = 1$$

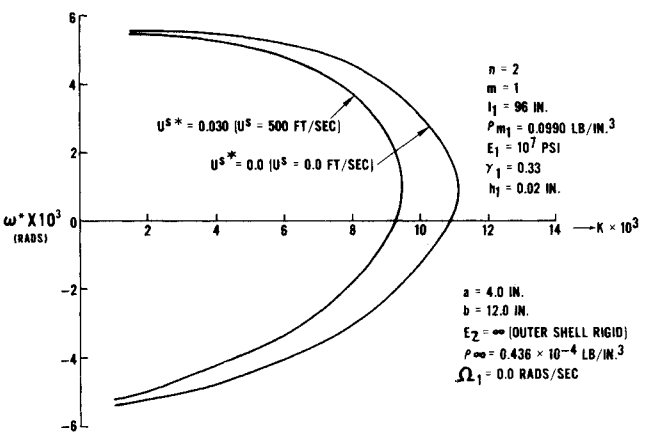

Fig. 2 Analytical solution for U^s = constant, $V^s = kr$, $W^s = 0$.

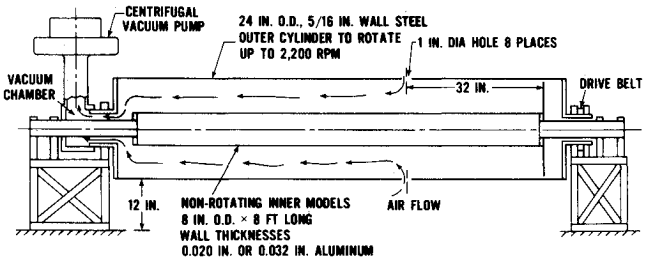

Fig. 3 Experimental model.

For $U_s = 0$ and V^s given by a profile of Fig. 4, attempt was made to integrate Eq. (20) for f_1, f_2 from $r = 1$ to $r = \delta$ by Runge-Kutta method. However, this leads to a numerical integration problem, when the coefficient of f'' becomes zero in the region of integration. Therefore, the following scheme was used to obtain the numerical results presented in this paper.

The solutions f_1, f_2 were obtained from Eqs. (6–9) by a finite difference scheme. These when expressed using $\tilde{p} = f(r)e^{i\beta}$ and similar expressions for $\tilde{u} = \tilde{u}(r)e^{i\beta}$ etc., result in four equations in $\tilde{u}(r)$, $\tilde{v}(r)$, $\tilde{w}(r)$, $\tilde{w}'$, f and f'. At $r = 1$, f and f' are known, enabling one to solve for the other four. Knowing $\tilde{w}'$ and f', $\tilde{w}(r)$, then f can be obtained at the next station, where one can solve for $\tilde{u}(r)$, $\tilde{v}(r)$, $\tilde{w}'$, and f', and the process repeated at each station.

The number of stations between $r = 1$ and $r = \delta$ were $(20 \times \delta)$, δ being 3 in this case. For each tangential velocity profile, a typical curve such as shown in Fig. 2, is obtained. This leads to one point on a curve of Fig. 5 or 6. The computing time needed to obtain each such point was about 30 sec. The calculations were performed on an IBM 370-168 computer.

Analytical Solutions, Special Cases

Analytical solutions have been obtained for two special velocity profiles. The first is for $U^s = U_\infty$ (constant), $V^s = k/r$, and $W^s = 0$ (K = constant). This flow condition is irrotational. Under the assumptions made for the fluid and by invoking Kelvin's Circulation Theorem,[7] it can be shown that the perturbed velocity field is also irrotational. Hence, the present

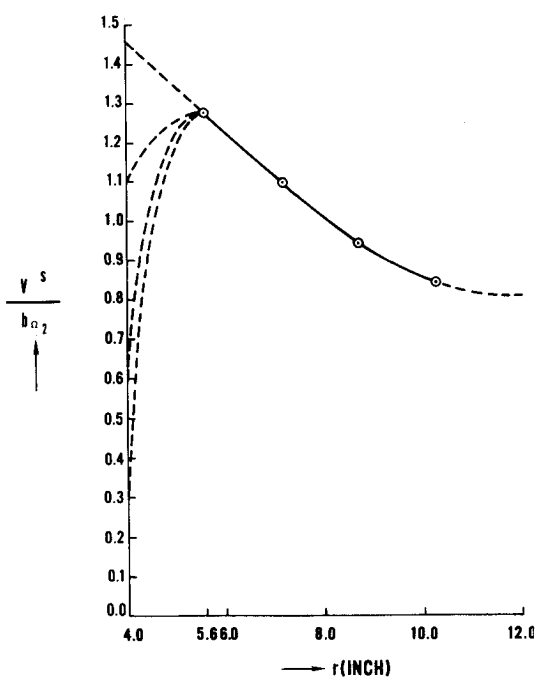

Fig. 4 Tangential velocity profile for test configuration.

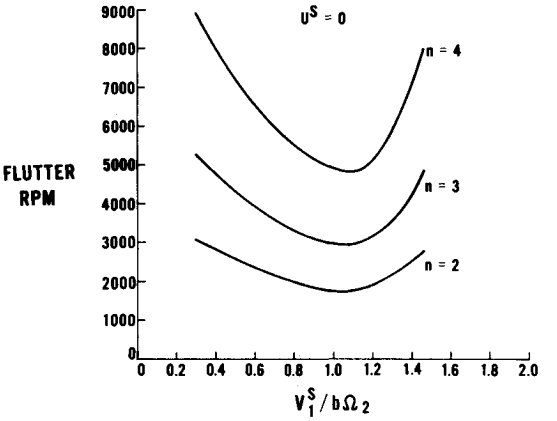

Fig. 5 Flutter rpm vs reduced velocity. Note: Measured flutter rpm 1800. $V_1^s b\Omega_2$ not measured. These plots are based on the measured tangential velocity profiles of Fig. 4; each is represented by its $(V_1^s/b\Omega_2)$.

theory should produce results identical to those for the incompressible case of Ref. 5. From Ref. 5 the perturbed pressure $\tilde{p}$ based on the unsteady Bernoulli's equation is

$$\tilde{p} \sim \alpha(r) \cdot \hat{\phi}(r) \tag{25}$$

where

$$\hat{\phi}''(r) + \frac{1}{r}\hat{\phi}'(r) - \left(\frac{n^2}{r^2} + \lambda^2\right)\hat{\phi}(r) = 0 \tag{26}$$

That Eq. (25) is indeed a solution of Eq. (20) can readily be checked by direct substitution.

The second solution is for $U^s = U_\infty$ (constant), $V^s = kr$, (k = constant), and $W^s = 0$. In this case, Eq. (20) reduces to

$$f'' + \frac{1}{r}f' + \left(-\frac{n^2}{r^2} + d\right)f = 0 \tag{27}$$

where

$$d \equiv \frac{\lambda^2}{\alpha^2}[-\alpha^2 + 4K^2]$$

with

$$\alpha = [-\omega + K_n + U_\infty \lambda] = \text{constant}$$

Solutions to Eq. (27) are

$$f = a_1 J_n[(+d)^{1/2}r] + a_2 Y_n[(+d)^{1/2}r] \quad \text{if} \quad |2K| > |\alpha|$$

or

$$f = a_1 I_n[(-d)^{1/2}r] + a_2 K_n[(-d)^{1/2}r] \quad \text{if} \quad |2K| < |\alpha| \tag{28}$$

or

$$f = a_1 r^n + a_2 r^{-n} \quad \text{if} \quad |2K| = |\alpha|$$

where J_n, Y_n, I_n, and K_n are standard Bessel functions, and a's are arbitrary constants.

Solution (28) is plotted in Fig. 2 as a function of K vs ω. For $U^{s*} = 0.0303827$ ($U^s = 500$ ft/sec), flutter occurs at $K = 9.5\times$

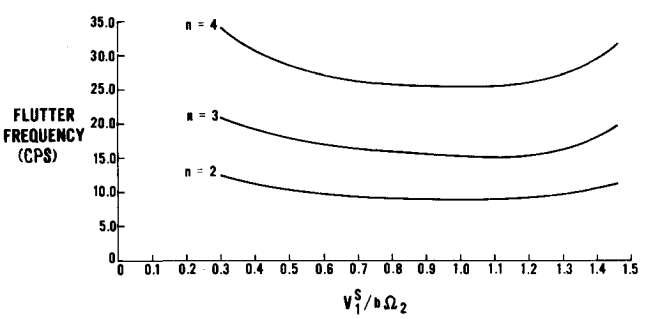

Fig. 6 Flutter frequency vs reduced velocity. These plots are based on the measured tangential velocity profiles of Fig. 4; each is represented by its $(V_1^s/b\Omega_2)$.

10^{-3} (giving $V^s = 156$ ft/sec at the inner shell) and $\omega^* = 1.1 \times 10^{-3}$ rads ($\omega = 8.6$ cps).

Discussion

The analysis presented in this paper can be used to determine possible flutter instabilities of a thin, uniform, long cylindrical shell rotating about its longitudinal axis. The fluid is assumed to be contained within the annulus, between two coaxial shells. Because of rotation of one or both shells, the surface of the inner shell can be subjected to flow conditions which include tangential velocities in addition to any axial velocities of the fluid. Such flow conditions may represent in a simplified form the fluid flow within the annulus of dual-spool rotor systems of jet engines. The axial velocity and tangential velocities of the fluid may have a general distribution within the annulus. It is the latter feature that distinguishes this analysis from that of Ref. 5, where a potential vortex profile was assumed for the tangential velocities within the annulus.

The problem is posed as follows. Given 1) all the structural characteristics of the shells, 2) fluid velocities (i.e., profile forms for the axial and tangential velocities), and 3) prescribed mode of vibration of the inner shell, what are the *magnitudes* of the tangential velocities (keeping the given profile forms geometrically similar) that will render the inner shell unstable? Once these magnitudes for the tangential velocities are determined, then the rpm of the outer shell may be calculated with due consideration given to the possible loss of fluid speed as it issues from the outer shell. Such an rpm is designated as "flutter rpm" and refers to the rotational speed of the outer cylinder at which the inner cylinder response becomes unstable. Thus, under given conditions stated above, the analysis determines the magnitude of the circumferential velocity which, when perturbed, leads to continuously increasing vibratory amplitudes (flutter) of the inner shell.

The method of computation is essentially similar to that described in detail in Ref. 5. For prescribed structural and fluid conditions, the eigenvalues representing the speeds of forward and backward traveling waves are computed. The given tangential velocities are repeatedly changed, but only in magnitude, preserving the given profile geometrically similar, until the wave speeds coincide or coalesce. The velocity distributions for the given profile at which coalescence occurs determines the required distribution of tangential velocities within the annulus. Based on the magnitude of the tangential velocity at the location of the outer cylinder, the "flutter rpm" can be computed. The ideal condition would be that when the tangential velocity of the fluid and that of the outer cylinder are the same. But in practice if the fluid issues from an outer cylinder through holes located on its periphery, some allowance would have to be made for possible losses. Therefore, the actual "flutter rpm" is likely to be more than that suggested by the ideal condition referred to above.

An experimental investigation of the type of flutter instabilities described here was conducted and the details of the results obtained are contained in Ref. 8. The principal parameters of physical interest which are used to compare theoretical and experimental results are 1) "flutter rpm" and 2) flutter frequency. The latter refers to the vibratory frequency at which the inner cylinder responds when flutter begins.

Typical results obtained for the test configuration shown in Fig. 3 are presented in Figs. 5 and 6. The structural and aerodynamic parameters for this configuration are the same as those listed in Fig. 2. The calculations were performed using the measured tangential velocity of Fig. 4. As measurements were made at only four locations within the annulus, the dotted lines shown in Fig. 4 represent possible extensions of the profile in the close vicinity of the inner shell. These possible extensions are represented by the parameter $V_1^s/(b\Omega_2)$. The results are plotted against this parameter. In calculating the "flutter rpm," a pick-up factor of 80% was used at the outer shell (ratio of V_2^s to outer shell velocity is 0.8). The experimental "flutter rpm" was 1800. Had the measurement been $V_1^s/b\Omega_2 = 1.1$, the present theory would predict accurately the experimental value for "flutter rpm." The results thus indicate that a definite improvement in the correlation between the predicted "flutter rpm" from this analysis and experimental observations is possible, provided measurements of the steady-state velocities include those in the close vicinity of the inner shell. However, there is poor correlation between the predicted flutter frequency ($\sim$10 cps) and the measured frequency ($\sim$65 cps).

Appendix: Derivation of Eq. (9) for $\tilde{p}$

By taking the divergence of Eqs. (6–8), i.e.,

$$\left(\frac{\partial}{\partial r}+\frac{1}{r}\right)(6)+\left(\frac{1}{r}\frac{\partial}{\partial\theta}\right)(7)+\left(\frac{\partial}{\partial z}\right)(8)$$

and using Eqs. (8) and (5) we get

$$-\nabla^2\tilde{p}=2\rho_\infty\left[\frac{1}{r}\frac{\partial V^s}{\partial r}\frac{\partial\tilde{w}}{\partial\theta}+\frac{\partial U^s}{\partial r}\frac{\partial\tilde{w}}{\partial z}-\frac{V^s}{r}\frac{\partial\tilde{v}}{\partial r}-\frac{\partial V^s}{\partial r}\frac{\tilde{v}}{r}\right] \quad \text{(A1)}$$

From Eq. (7)

$$-[B]\tilde{v}-\frac{1}{\rho_\infty r}\frac{\partial\tilde{p}}{\partial\theta}=[A]\tilde{w} \quad \text{(A2)}$$

From Eq. (6)

$$[B]\tilde{w}-2\frac{V^s}{r}\tilde{v}=-\frac{1}{\rho_\infty}\frac{\partial\tilde{p}}{\partial r} \quad \text{(A3)}$$

Substitution of $\tilde{w}$ from Eq. (A2) into Eq. (A3) and use of Eq. (5) gives

$$\left[B^2+\frac{2V^s}{r}A\right]\tilde{v}=-\frac{1}{\rho_\infty r}[B]\frac{\partial\tilde{p}}{\partial\theta}+\frac{1}{\rho_\infty}[A]\frac{\partial\tilde{p}}{\partial r} \quad \text{(A4)}$$

Substituting $\tilde{w}$ of Eq. (A2) into Eq. (A1), and using Eq. (5) we get

$$[A]\left(-\frac{\nabla^2\tilde{p}}{2\rho_\infty}+\frac{V^s}{r}\frac{\partial\tilde{v}}{\partial r}=\frac{\partial V^s}{\partial r}\frac{\tilde{v}}{r}\right)=-\frac{1}{r}\frac{\partial V^s}{\partial r}[B]\frac{\partial\tilde{v}}{\partial\theta}-$$
$$\frac{\partial U^s}{\partial r}[B]\frac{\partial\tilde{v}}{\partial z}-\frac{1}{\rho_\infty r^2}\frac{\partial V^s}{\partial r}\frac{\partial^2\tilde{p}}{\partial\theta^2}-\frac{1}{\rho_\infty r}\frac{\partial U^s}{\partial r}\frac{\partial^2\tilde{p}}{\partial\theta\,\partial z} \quad \text{(A5)}$$

Equations (A4) and (A5) are in $\tilde{v}$ and $\tilde{p}$ only. Substituting $\tilde{v}$ from Eq. (A4) into Eq. (A5), and using Eq. (5) we get (10) for $\tilde{p}$.

References

[1] Leonard, R. W. and Hedgepeth, J. M., "On Panel Flutter and Divergence of Infinitely Long Unstiffened and Ring-Stiffened Thin-Walled Circular Cylinders," TR 1302, 1957, NASA.

[2] Miles, J. W., "Supersonic Flutter of a Cylindrical Shell," *Journal of the Aeronautical Sciences*, Vol. 24, No. 2, Pt. I, Feb. 1957, pp. 107–118.

[3] Bolotin, V. V., *Nonconservative Problems of the Theory of Elastic Stability*, Macmillan, New York, 1963.

[4] Dowell, E. H., "The Flutter of an Infinitely Long Cylindrical Shell," Aeroelastic and Structures Research Lab., MIT; also TR 112-3, Air Force Office of Scientific Research 65-0639, Jan. 1965.

[5] Srinivasan, A. V., "Flutter Analysis of Rotating Cylindrical Shells Immersed in a Circular Helical Flowfield of Air," *AIAA Journal*, Vol. 9, No. 3, March 1971, pp. 394–400.

[6] Wilson, B., "A Geometrically Nonlinear Theory of Shells," TR 32-584, 1963, Jet Propulsion Lab., Pasadena, Calif.

[7] Emmons, H. W., ed., *Fundamentals of Gas Dynamics, Vol. III, High Speed Aerodynamics and Jet Propulsion*, Princeton University Press, Princeton, N.J., 1958.

[8] Dowell, E. H. and Srinivasan, A. V., McLean, J. D., and Ambrose, J., "Aeroelastic Stability of Cylindrical Shells Subjected to a Rotating Flow," *AIAA Journal*, Vol. 12, No. 12, Dec. 1974, pp. 1644–1651.